remote sensing

Article

Snow Avalanche Hazard Mapping Using a GIS-Based AHP Approach: A Case of Glaciers in Northern Pakistan from 2012 to 2022

Afia Rafique [1], Muhammad Y. S. Dasti [2], Barkat Ullah [3,*], Fuad A. Awwad [4], Emad A. A. Ismail [4] and Zulfiqar Ahmad Saqib [5,6]

1 Department of Meteorology, Comsats University, Islamabad 45550, Pakistan; sp20-rrg-001-@isbstudent.comsats.edu.pk
2 School of Geo-Sciences and Info-Physics, Central South University, Changsha 410012, China; yousafsardardasti@gmail.com
3 School of Resources and Safety Engineering, Central South University, Changsha 410083, China
4 Department of Quantitative Analysis, College of Business Administration, King Saud University, Riyadh 11587, Saudi Arabia; fawwad@ksu.edu.sa (F.A.A.); emadali@ksu.edu.sa (E.A.A.I.)
5 Institute of Soil and Environmental Sciences, University of Agriculture, Faisalabad 38040, Pakistan; zulfiqar.dasti@uaf.edu.pk
6 Agriculture Remote Sensing Lab, National Centre for GIS and Space Application, Islamabad 44000, Pakistan
* Correspondence: barkat_ullah@csu.edu.cn

Abstract: Snow avalanches are a type of serious natural disaster that commonly occur in snow-covered mountains with steep terrain characteristics. Susceptibility analysis of avalanches is a pressing issue today and helps decision makers to implement appropriate avalanche risk reduction strategies. Avalanche susceptibility maps provide a preliminary method for evaluating places that are likely to be vulnerable to avalanches to stop or reduce the risks of such disasters. The current study aims to identify areas that are vulnerable to avalanches (ranging from extremely high and low danger) by considering geo-morphological and geological variables and employing an Analytical Hierarchy Approach (AHP) in the GIS platform to identify potential snow avalanche zones in the Karakoram region in Northern Pakistan. The Advanced Space-borne Thermal Emission and Reflection Radiometer (ASTER) Global Digital Elevation Model (GDEM) was used to extract the elevation, slope, aspect, terrain roughness, and curvature of the study area. This study includes the risk identification variable of land cover (LC), which was obtained from the Landsat 8 Operational Land Imager (OLI) satellite. The obtained result showed that the approach established in this study provided a quick and reliable tool to map avalanches in the study area, and it might also work with other glacier sites in other parts of the world for snow avalanche susceptibility and risk assessments.

Keywords: susceptibility analysis; avalanche; risk reduction strategies; ASTER GDEM; risk assessments; geo-morphological

Citation: Rafique, A.; Dasti, M.Y.S.; Ullah, B.; Awwad, F.A.; Ismail, E.A.A.; Saqib, Z.A. Snow Avalanche Hazard Mapping Using a GIS-Based AHP Approach: A Case of Glaciers in Northern Pakistan from 2012 to 2022. *Remote Sens.* **2023**, *15*, 5375. https://doi.org/10.3390/rs15225375

Academic Editors: Gareth Rees, Jiahua Zhang, Alex Okiemute Onojeghuo and Fengmei Yao

Received: 21 August 2023
Revised: 30 October 2023
Accepted: 1 November 2023
Published: 16 November 2023

1. Introduction

In recent years, global warming has increased due to many anthropogenic activities, and consequently, frequent and unusual calamities associated with temperature, rainfall, and snowfall sometimes turn into stern natural disasters [1]. Snow avalanches are a well-known hazard type and are defined as a sudden release of snow masses and ice from slopes, sometimes containing portions of rocks, soil, and vegetation, damaging lives, infrastructure, and ecosystems and, thus, are considered 'white death' in glacier regions [2]. Avalanche is a natural phenomenon that develops because of a complex interaction between snowpack, terrain, and meteorological conditions [3], commonly occurring during or after heavy snowfall [4]. After snowfall, more new layers of snow develop that add more weight to the existing snow layers, which are called snowpack [5], and this large mass of snow slips down through a steep slope and gathers the snow in its path, thus resulting in the development of 'avalanches'. Many avalanche incidents have happened over the last thirty years and impacted approximately 70,000 individuals and communities [6]. The northern region of Pakistan lies within the mountainous range of the Karakoram and Hindu Kush Himalayan range and has several of the longest glaciers present in polar places like Siachen, Hispar, Baltora, Batura, Yenguta, Chianti, Trich, and Atrak. Three of the world's seven largest glaciers are in Pakistan's northern region [7].

Due to the inaccessibility of this region, conducting field surveys and evaluating avalanche activity are difficult tasks [8]. Climate change has serious impacts, resulting in the melting of glaciers globally as well as in Hindu Kush, Himalayas, and Karakoram, and their melting rate has been increasing over time due to the rise in mean temperature by 0.6 °C in Pakistan between 1901 and 2007 [9]. Rising temperatures are rapidly melting glaciers in Pakistan's northern mountain ranges and have resulted in the formation of 3044 glacial lakes in this area (UN Report). The major incidents and loss of lives from 2010 to 2022 are presented in Table 1, while the damage to infrastructure caused by these incidents is frequent and even larger (Figure 1). In recent years, the area received its heaviest snow spell in its 100-year history, isolating the region from the rest of the country [1]. To create an inventory of glacier types and measure ice reserves in the area, a basic understanding of the historical activities of glaciers is imperative, especially for studying their surge mechanisms. Overall, this area represents a region with a high potential for snow avalanche occurrences, and understanding the relationship between glaciers and avalanches in this area is crucial for formulating effective risk assessment and mitigation strategies.

Table 1. Avalanche accidents and associated fatalities in the study area.

Date/Year	Latitude	Longitude	Type	Fatalities	Source
16 February 2010	35.41191	72.94035	Snow Avalanche	120	
4 July 2012	35.49801	76.75336	Ice and Rock Avalanche	140	[10]
14 January 2020	34.82701	74.35855	Snow Avalanche	65	

Figure 1. The occurrence of snow avalanches and damage due to snow avalanches in the study area.

The development of avalanche susceptibility maps is an important step in determining avalanche risk and preventing the loss of life and property. It helps decision makers and planners to implement appropriate avalanche risk reduction strategies. AHP has most often been used in the production of avalanche susceptibility maps using multiple static terrain criteria (elevation, slope, aspect, and curvature) [2,4]. The use of satellite remote sensing in conjunction with the AHP technique ensures the formulation of a comprehensive and scientifically rigorous approach to studying such phenomena [11]. GIS-based Multi-Criteria Decision Analysis (MCDA) using the AHP model (MCDA-AHP) based on hierarchical weighing was conducted to develop a comprehensive avalanche susceptibility map of these glaciers in Pakistan. This will help us to understand hazard factors and devise and implement effective mitigation measures.

2. Materials and Methods

2.1. Study Area

The study was conducted in the Karakoram–Himalaya mountain range, located between the borders of Pakistan, India, China, and Afghanistan, and stretches over ∼500 km in a NW to SE direction (Figure 2). The region includes four peaks higher than 8000 m a.s.l and some of the largest glacier exteriors in the polar region, such as Siachen, Hispar, Baltoro, Batura, Yenguta, Chiantar, Trich, and Atrak. Three out of seven of the world's biggest glaciers are in Pakistan. The Karakoram range in the region is particularly prone to avalanches due to its rugged topography, high altitudes, and abundant snowfall. This mountain range is host of all three glaciers under this study (Figure 2). The Hispar Glacier (36°04′60″N and 75°15′60″E) is in central Karakoram, stretching over 53 km and spans larger than 500 km^2 with a height range of around 3100–7500 m (https://documents.worldbank.org/curated/pt/127761468197388108/pdf/67668-WP-Glacier-Report-PUBLIC.pdf, accessed on 31 October 2023). The Hispar Glacier is influenced by the long rainy season, with significant melting from late June to early October [12], and comprises both pure and particulate ice supraglacial lakes. The Saltoro Mountains are also known as a modularization of the Karakoram Mountains that encompass the Gayari Glacier (35°12′49″N and 77°06′34″E). It is in the middle of the Karakoram, on the other side of the Siachen Glacier, one of the world's longest glaciers outside of the polar regions. The valley's temperature fluctuates between 14 °C and 34 °C in the summertime but drops to −50 °C in the wintertime and reaches 10 m of snowfall, with an annualized rate of 6–7 m. Snowstorms travel at rates of up to 300 km/h [12]. The Batura Glacier is situated in Pakistan's Gilgit-Baltistan area, in the upper Hunza Valley (36°31′59″N, 74°38′59″E), as shown in Figure 1, and is also roughly 57 km long. Batura Glacier is situated directly north of the Batura Muztagh, a sub-range of the Karakoram mountain range that comprises the quartiers of Batura Sar (7795 m), the 25th highest peak on Earth.

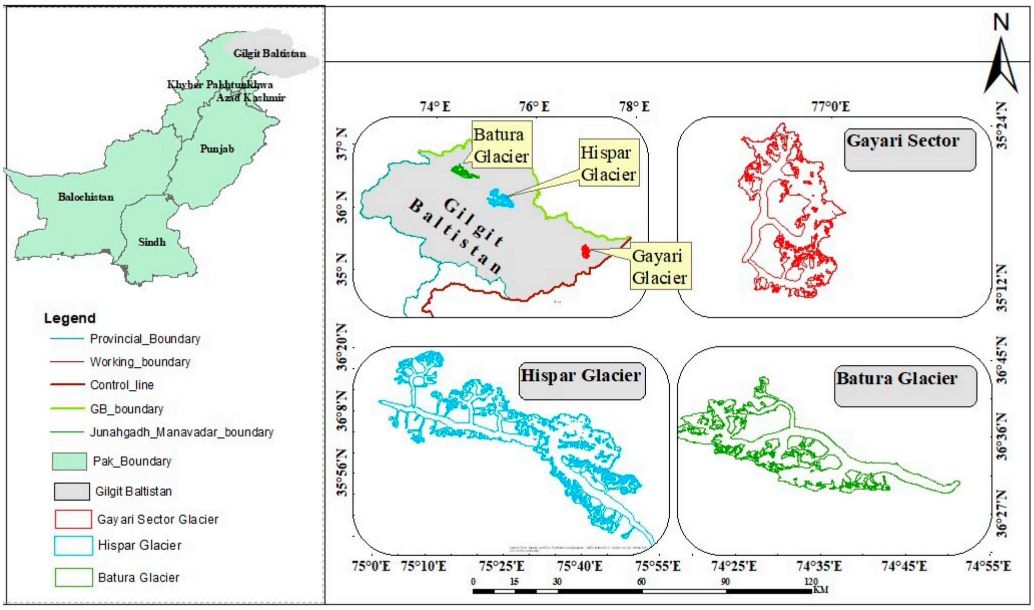

Figure 2. The study area map represents the location of Hispar, Gayari Sector, and Batura Glacier.

2.2. Methodology Chart

Reliable inventory and data are essential for such studies, as data availability is very difficult in such areas. The six factors were chosen based on their significance to avalanche occurrences, as well as availability of data. The flow chart of the research framework is shown in Figure 3. The avalanche susceptibility map was split to use the natural breaks, i.e., Jerks' method, divide the population into four susceptibility thresholds: very low, low, high, and very high.

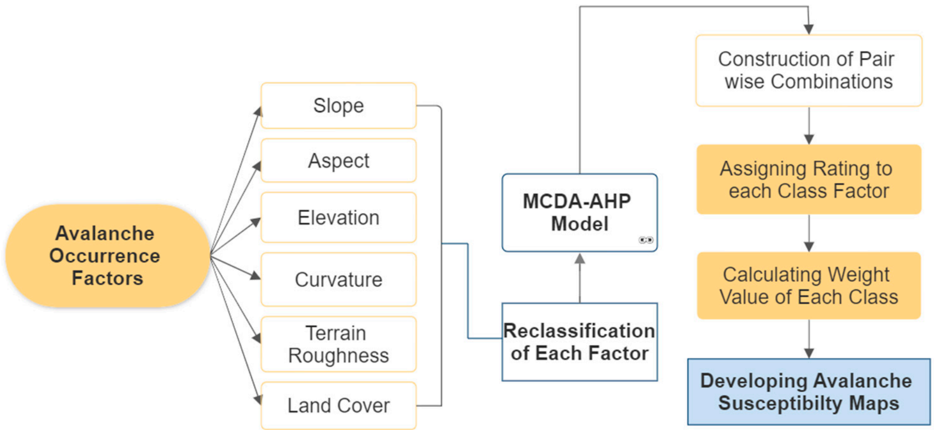

Figure 3. Flowchart representation of the research methodology used.

2.3. *Remote Sensing and Ground Data*

Satellite images are always regarded as the first option for data acquisition in glacier avalanche investigations due to ease of availability, coverage, and excellent spatial, spectral, and temporal resolutions. Two remote sensing satellite instruments, Landsat 5 (TM) and Landsat 8 (OLI), were utilized as remote sensing data sources for the assessment of avalanche susceptibility in glaciers during the last ten years from 2012 to 2022. The data characteristics of these satellites are provided in Table 2.

Table 2. Satellites and characteristics of data used in the study area.

Locations	Year	Satellite	Spectral Resolution	Spatial Resolution (m)	Cloud Coverage
Hispar, Batura, Gayari Glaciers	2012 2022	Landsat 5 (TM) Landsat 8 (OLI)	1–7 1–7	30 × 30 30 × 30	0–5% 0–5%

The first form of the remotely sensed data used was the Digital Elevation Model (DEM), which is regarded as an essential input in glacier avalanche research modeling. The Terra Advanced Space-borne Thermal Emission and Reflection Radiometer (ASTER) and Global Digital Elevation Model (GDEM) with 30 × 30 m resolution were derived and downloaded from USGS Earth Explorer (https://earthexplorer.usgs.gov, accessed on 24 May 2023).

2.4. *Evaluation of Avalanche Impact Variables and Formation of Thematic Layers*

The structure and stability of the snowpack are determined by consecutive snowfall under meteorological circumstances. The bulk of avalanches arise when the snowpack becomes too weak to maintain its material or when other pressures (natural or anthropogenic) surpass the snowpack's strength. Avalanche activity is influenced by meteorological parameters such as snowfall, temperature, wind speed, wind direction, and precipitation, as well as elevation, terrain roughness, and ground snow cover [13,14]. Overall, important characteristics of avalanche occurrence in terrain include aspect, slope, land cover, terrain roughness, elevation, and curvature. Each one of these factors is taken as a data layer and is discussed below.

2.4.1. Slope

The occurrence of avalanches depends on the steepness of the slope. They are triggered when the slope angles meet a specific range. Generally, snow avalanches start from terrain that is steeper than about 30°–45°; however, they can initiate on a mild slope of 25° as well as steep slope of 60° [3]. When the slope exceeds an angle of 45°, the chances of avalanches increase because snow cannot be retained effectively [12]. This means that most skier-triggered avalanches happen on slopes that are 30° to 45° [15].

2.4.2. Aspect

The angle of the slope of the terrain surface is designated as an aspect that has a direct influence on snow destabilization. The stability of snowpack is largely affected by the orientation of slopes with respect to the sun. The reported data of the Austrian and Swiss areas indicate that 50% of all avalanches occur on the northern side (NW–E–NE) of the aspect [16]. Slopes that are in shadow (dark slopes) receive little radiant energy, and for this reason, they remain frozen. In general, north-facing slopes of the northern hemisphere are characterized by strong temperature gradients, thus forming weak layers of snow or poor snow strata [12]. Thus, aspect metadata layer was used and divided into nine classes: N, NE, SE, S, SW, W, NW, and Flat for this study.

2.4.3. Elevation

Elevation does have a strong association with the occurrence of avalanche-origin zones. At higher elevations, meteorological parameters (precipitation, temperature, and wind) are highly linked with avalanche formation and initiation in such areas.

2.4.4. Curvature

The other essential element promoting avalanche is curvature, which represents shape of the slope. Slopes are generally classified as concave, convex, or flat curvatures. Although avalanches can occur in any type of curvature, concave slopes have a higher avalanche potential than convex and flat slopes [17]. The curvature also influences the speed of the snow flow or shift. Straight slopes cause higher acceleration in snow mass after avalanche occurs, while convex curvature produces stress in the glacier, which promotes shearing and break instability and, as a result, increases chances of initiation of avalanches. Concave curvature, on the other hand, causes avalanche deformation, which helps prevent minor rock avalanches. In this study, curvature raster was reclassified into 3 classes: concave (<-0.2), flat (-0.2–0.2), and convex ($0.2<$). This classification represents terrain features based on their curvature values.

2.4.5. Terrain Roughness

The roughness of the terrain underneath the snowpack is decisive for the occurrence of snow gliding and subsequent wet-snow avalanches. Roughness can act as a stabilizing factor [18]. Grassy, abandoned meadows are especially prone to snow gliding, while fallen logs, snapped trees, and large rocks can prevent the formation of small avalanches by supplying structural support, but not extreme ones. This computation is carried out for each cell in the DEM.

2.4.6. Land Cover

Avalanche occurrences are also affected by the kind of land cover. Because ice/snow cover and barren slopes are more vulnerable to snowpack instabilities than places with plants. The greatest value was awarded to ice/snow cover followed by bare, rocky, and moraines slopes.

2.5. MCDA-AHP Model

AHP is applied to compute the evaluations of varying factors based on their importance to decision makers. This approach is based on the examination of 2 factors in pairs. The AHP model was constructed by Saaty in 1980 [19], and one of the important advantages of the AHP model is its ability to evaluate quantitative as well as qualitative criteria and alternative approaches in an equal order to accommodate differences [20]. An AHP approach tackles decision-making difficulties by organizing them in a hierarchy [21].

For the primary phase when employing the AHP model [22], the first step is to identify the unstructured problem and decide what kind of material is needed. Begin at the top with the objective and make your way through different levels to the least number in 2nd step. In 3rd step, a pairwise ranking system of a set of criteria is created utilizing Saaty's importance scale (Table 3) to estimate eigenvectors and eigenvalues.

Table 3. Saaty's scale of AHP relative importance value.

Importance	Definition	Explanation
1	Equal Importance	Contribution to the objective is equal
9	Extreme Importance	One attribute is of the highest possible order of affirmation
3	Moderate Importance	The attribute is slightly favored over another
5	Strong Importance	The attribute is strongly favored over another
7	Very Strong Importance	The attribute is very strongly favored over another
2, 4, 6, 8	Intermediate Values	When compromise is needed

The consistency of the entire decision-making process in AHP depends on the consistency of the individual comparisons made by the decision maker in compliance with the criteria. Whether the comparisons are consistent is evaluated by the consistency ratio (CR). CR was calculated using the method established by Saaty (1988) [23] and provided in Equation (1). CR is determined to assess the coherence with the pairwise comparison matrix, and it ought to be below 0.1.

$$\mathrm{CR} = \frac{\mathrm{CI}}{\mathrm{RI}} \tag{1}$$

Here, *CI* stands for consistency index, and RI stands for random consistency index. The consistency index defines the departure from coherence, as in Equation (2).

$$CI = \frac{\lambda_{\mathrm{max}} - \mathrm{n}}{\mathrm{n} - 1} \tag{2}$$

While λ_{max} is the greatest component, N is the comparability matrix's value. The consistency index should not exceed 0.1 or 10%. For RI, the judgment-based preferences were applied to rate the priority at the level for each component; following Table 4 calculate and sum their evaluation values to figure out their total priority.

Table 4. Random consistency index.

N	1	2	3	4	5	6	7	8	9	10	11	12	13	14	15
R	0	0	0.5	0.9	1.1	1.2	1.3	1.4	1.4	1.4	1.5	1.5	1.5	1.5	1.5
I	0	0	8	0	2	4	2	1	5	9	1	3	6	7	9

The result is a combination of factor weighting and factor prioritization rankings. The factor weight values in the pairwise comparison matrix were determined, and the resultant values were obtained using Equation (3).

$$Z = \sum_{j=1}^{n} (WiXi) \tag{3}$$

2.6. Avalanche Susceptibility Mapping

The MCDA-AHP model was used in ArcGIS platform to generate avalanche susceptibility maps for three glaciers. The evaluation provided for each class of parameters is based on known avalanche sites. The avalanche occurrence factors were determined using a pairwise comparison matrix, and the centroid values were determined; then, the occurrence factors were scored on a scale of 1 to 9. The weight values of the factors were calculated after the pairwise comparison matrix. The CR value is utilized in the MCDA-AHP model to reflect the regularity of the pairwise comparison matrix assessments, and it should be less than 0.1.

Avalanche susceptibility index (*ASI*) was calculated using Equation (4), which is the summation of the avalanche factors. Each factor is multiplied by its corresponding weight, and these products are then summed to obtain the *ASI*, providing a comprehensive assessment of avalanche susceptibility.

$$ASI = \sum_{i=1}^{n} (0.40 \times S) + (0.28 \times C) + (0.14 \times A) + (0.09 \times TR) + (0.05 \times E) + (0.03 \times GC) \quad (4)$$

where *S*, *C*, *A*, *TR*, *E*, and *GC* represent slope, curvature, aspect, terrain roughness, elevation, and ground cover.

3. Results

3.1. Hispar Glacier

The avalanche-forming characteristics of the Hispar Glaciers were studied while determining the avalanche occurrence parameters, and this aspect is taken as a major consideration when evaluating any avalanche risk regions [18]. Most of the avalanche terrain within the research region faces north and remains dangerous year-round. The windward slopes consolidate snow comparably quickly, while the lower-side slopes take longer [24]. ASTER GDEM V3 is used to create an aspect, which is then divided into nine groups. North and southeast classes were found more vulnerable to avalanche occurrence (Figure 4), as observed in other studies [25].

In general, it is recognized that most of the avalanche activity happened at slope angles ranging from 30° to 50°. The slope of the glacier ranges from 28° to 60°, depending on snow thickness and water level [15]. The slope inclination influences the probability and amplitude of avalanches. Because of erosive or geo-morphological circumstances, slope inclination is also influenced by vegetation cover [13]. The slope was derived by using the adaptation of cell values to their neighbors in ASTER GDEM V2. The slope data were then categorized into five groups and used in the current structure. The terrain has an indirect effect on the incidence of snow avalanches. With increasing altitude, the density of snowfall rises. During the winter period, the high-altitude regions receive the highest snowfall and snow cover. Rain may fall at lower altitudes at the start of the winter season and throughout the spring. Wind velocity frequently increases with elevation, and so does the volume of snow supplied by the air [26]. The ASTER GDEM V2 was classified into six elevation classes with elevation differences ranging from 3800 to 6200 m (Figure 4).

Another avalanche-contributing factor is curvature [27]. Avalanches are more prevalent on convex slopes, but they can occur on concave and flat slopes as well. In ASTER GDEM V2, curvature was determined by computing the second derivative of the elevation values with respect to the x and y coordinates of each source cell, considering the cell's area. This process allowed for the characterization of terrain features based on their convex or concave curvature. A curvature map was generated and classified into three categories: Concave, Flat, and Convex (Figure 4); however, flat curvature was dominant in the study area. Convex regions accelerate the downward motion of snow cover and are regarded as fragile, whereas concave regions are regarded as sturdier. Plains have a moderate impact on the incidence of snow avalanches.

Roughness can act as a stabilizing factor [15]. The terrain roughness restricts the snowpack's continuous slide and prevents the formation of a continuous tiny depth, which is truly required for major avalanche breaking [5]. Grassy, abandoned lands create a favorable environment for avalanche formation [28,29], while fallen logs, snapped trees, and large rocks provide structural support to check minor avalanches but are not effective for big ones. Avalanche susceptibility classification based on roughness assesses terrain features. Class 1 signifies low roughness with gentle slopes and sparse vegetation. Class 2 has slightly rougher terrain with gentle slopes and some vegetation. Class 3 has moderately rough terrain with mixed vegetation. Class 4 has steep slopes and dense vegetation, while Class 5 features extremely steep slopes and dense, potentially impenetrable vegetation, creating significant snow flow obstacles. Higher roughness reduces avalanche likelihood; lower roughness increases susceptibility. Overall, terrain roughness was categorized as 'low'. The incidence of avalanches is also determined by the kind of land cover. Ice/snow cover and bare slopes are far more vulnerable to avalanche structural instability than vegetation [30]. The study area is not diverse in this regard; thus, the land cover was divided into two types of ice/snow and others, which include stony, bare, and mountain ranges, as shown in Figure 4.

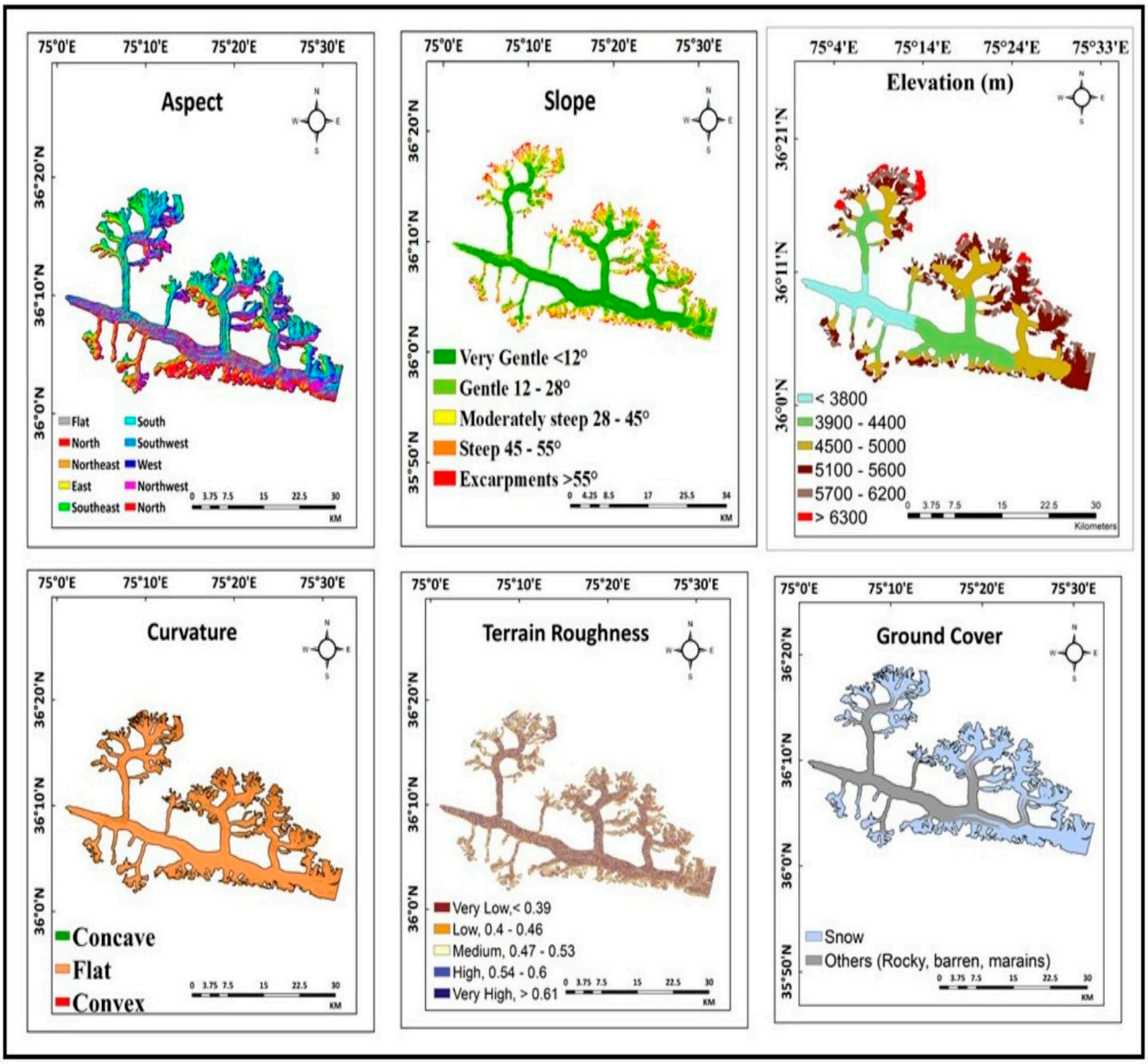

Figure 4. Thematic layers of avalanche occurrence factors at Hispar Glacier.

3.2. Batura Glacier

Aspect is regarded as among the most important aspects of avalanche development [13]. Aspect does have a significant influence on the snowpack's everyday durability in Batura Glacier. The characteristics and distribution of dark slopes or weak layers can be crucial for assessing avalanche susceptibility. Weak or unstable layers within the snowpack can contribute to avalanche initiation and propagation [30]. This is because the exposure to the sun is lower in that direction, which causes the snowpack to become more active.

The direction of the wind also helps in the accumulation of snow on these slopes. Other directed slopes encounter the sun's rays, which causes the melting of snow and reduces the susceptibility of avalanches [18]. Furthermore, breezy slopes are sustained by less snow than downwind slopes with greater snow masses, which might enhance the probability of avalanches [15,22,31]. Figure 5 shows that the aspect is classified into nine groups, and the south and north aspect was found to be more prone to avalanche occurrence.

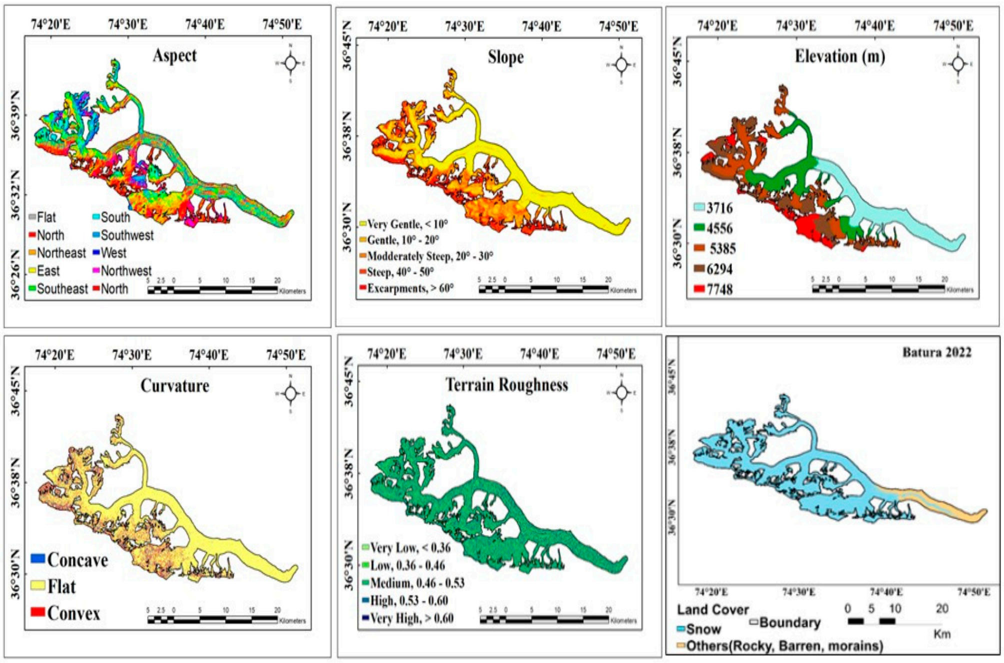

Figure 5. Thematic layers of avalanche occurrence factors at Batura Glacier.

The Batura Glacier is situated in the upper Hunza Valley in the Gilgit-Baltistan area of Pakistan. Six avalanche-forming characteristics were studied while determining the avalanche occurrence parameters. It is reported that avalanches typically occur on slopes at 28° and 45° [4,32]. The slope is derived using the adaptation of cell values to their neighbors in ASTER GDEM V2. The slope data are then categorized into five groups, with 40° to 50° slopes receiving the highest grade and <10° slopes receiving the lowest, as shown in Figure 5.

Elevation does not really enhance the likelihood of an avalanche happening. Yet, it is, indeed, closely related to climate characteristics that raise the danger of avalanches, including wind direction, temperature, snowfall level, and rainfall [27,31,33]. As elevation increases, temperatures lower, snow remains accessible for avalanches for a longer amount of time (this study includes both the lowest and highest altitudes of 3716 and 7748 m (Figure 5)), and higher altitudes have more susceptibility for avalanches in the region.

Curvature is regarded as an important factor in avalanche identification. Avalanches are more likely to happen on convex slopes because of glacier fragility than on concave or flat slopes, but they can happen on both [32]. In this study, the curvature is divided into three classes, as indicated in Figure 5d, and unlike the Hispar Glacier, there was variation in the curvature of the area.

The roughness of a setting may consequently have a detrimental influence on snowfall by adding stress and intensifying snow ablation processes throughout rugged terrain. Values between rough surfaces and smooth surfaces cause snow avalanches. The ruggedness method is employed to determine terrain roughness in this research [3]. Overall roughness values in the research region are divided into five groups and indicate the very low to very high values of terrain roughness, as shown in Figure 5. The importance of ground cover in avalanche incidence has been discovered. The ground cover in the current research region is devoid of vegetation and consists mostly of stony mountain ranges, batten areas, and other bare areas. Similarly, the current research region's land cover is divided into two categories, snow and others (barren, rocky, moraines), which clearly shows the higher snow coverage at Batura Glacier (Figure 5).

3.3. Gayari Sector Glacier

Aspect is an important factor in determining avalanche vulnerability. The sun-facing side has become steadier quite rapidly after a short duration of instability, but the shaded slopes stay unstable for a longer period. ASTER GDEM generated an aspect map, which is also divided into numerous classes, as illustrated in Figure 6a. Because the north and northeast classes received the highest rating, the majority of avalanche slopes in the research region face north and remain risky all year. Although altitude has little significant impact on avalanche initiating, this does affect snowfall, wind velocity, and temperature, each of which has an impact on snow avalanches.

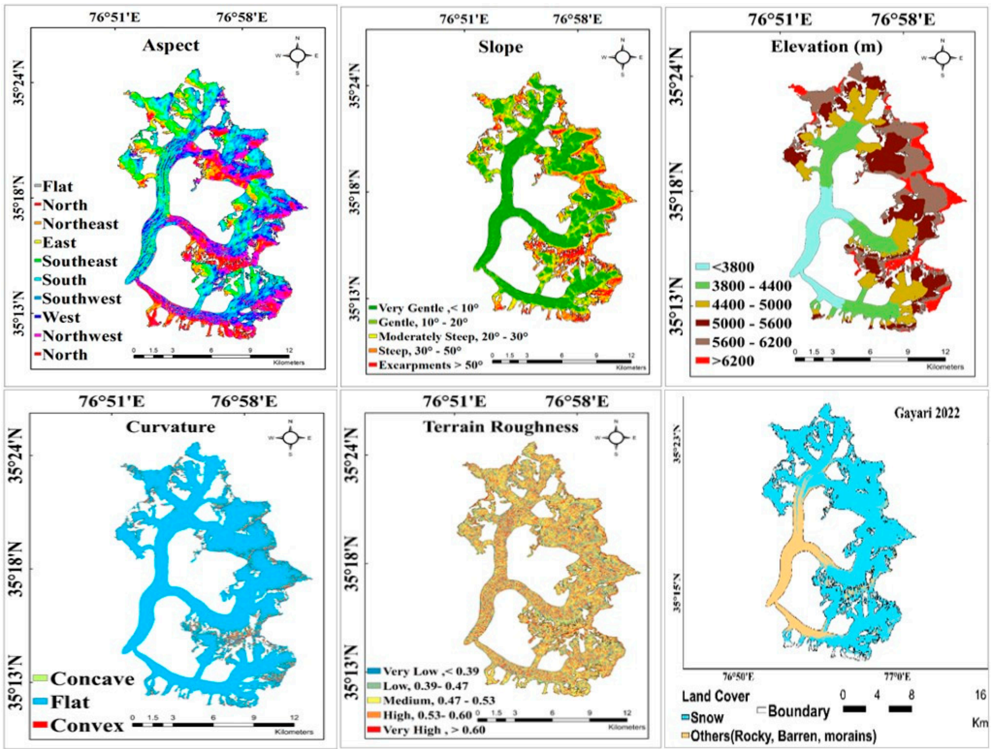

Figure 6. Thematic layers of avalanche occurrence factors at Gayari Glacier.

Avalanches originate on slopes exceeding 30°, with only a few occurring on slopes just under 25°. The force that tends to occur on these slopes is usually too low to cause an avalanche [34]. Because the quantity of snow accumulation on steep slopes (45–55°) is quite low, minor avalanches are common on these slopes. The slope map was constructed using ASTER GDEM and divided into five categories, as shown in Figure 6b. The >50° class received the highest slope, while the <10° class received the lowest.

Snow at lower elevations generally begins to melt due to warm, moist air. Avalanches have been documented between 2700 and 6000 m in the Indian Himalayas, with most avalanches occurring between 5000 and 5600 m in the higher Himalaya zone. The height of the research region ranges from 3832 to 7236 m. The formation zone of all dangerous avalanches in the research region, meanwhile, is over 5100 m. The elevation was divided into five categories, as shown in Figure 6c.

Curvature describes the morphology of the slope. Convex slopes promote snow cover fragility, whereas concave slopes aid in snow cover stabilization [17]. The curvature map was created using ASTER GDEM and divided into three types, Convex, Flat, and Concave, as illustrated in Figure 6d. The convex curvature received the most importance, the concave had the lowest importance, and the flat received a medium amount of importance.

The roughness of a setting may consequently have a detrimental influence on snowfall by adding stress and intensifying snow ablation processes throughout rugged terrain. The roughness of the environment may, therefore, have a negative impact on snowfall by causing additional stress and boosting snow-melting activities along rocky terrain. The MCDA-AHP approach and its application to mapping avalanche susceptibility are classified into five categories, which indicate very low roughness at <0.39 and very high roughness at >0.60, as shown above in Figure 6e.

The extensive forest cover reduces the consequences of avalanches. By keeping the snow mostly on the slopes, plant cover could restrict the quantity of snow accessible for avalanches. The higher Himalayan region's land cover is indeed not conducive to reducing the risk of snow avalanches. The land cover in the current research region is devoid of vegetation and consists primarily of stony moraines, barren areas, and other bare areas. The current research area's land cover is classified as snow and others (rocky, moraines, barren), as illustrated in Figure 6f, which indicates that the year 2012 has more snow cover than the year 2022.

3.4. Snow Avalanche Susceptibility

Avalanche susceptibility assessment necessitates an examination of both topographical and climatic factors. The ASTER GDEM V2 and Landsat 8 images are utilized to establish many inputs and topographical characteristics for avalanche susceptibility mapping using curvature, slope, elevation, aspect terrain roughness, and ground cover. According to their importance, each factor was defined and rated numerically (Table 5), and finally, priorities were synthesized for each layer through a pairwise comparison matrix with weight values using the MCDA-AHP approach, as shown in Table 6. The ASI is divided into four susceptibility perimeters (very low, low, high, and very high) to produce an avalanche susceptibility map of the study area using the AHP method, as presented in Figure 7. The zones of avalanche vulnerability, the slope with high peaks in comparison to where the slope peak is visible and where we have an extremely low slope, is the major determinant in avalanche risk.

Table 5. Assigning the ratings for each thematic layer/criterion.

Thematic Layer	Category	Rating	Weight
Slope	<20°	1	0.40
	12–28°	3	
	28–45°	9	
	45–55°	5	
	>55	3	
Elevation (m)	<3800	1	0.05
	3800–5000	3	
	5000–5600	7	
	5600–6200	5	
	>6200	2	
Aspect	Flat	1	0.14
	North or Northeast	9	
	East or South	3	
	Southeast	5	
	West and Southwest	2	
	Northwest	7	
Curvature	Concave	2	0.28
	Flat	3	
	Convex	5	
Terrain Roughness	<0.39	2	0.09
	0.39–0.46	5	
	0.46–0.53	4	
	0.53–0.60	7	
	>0.61	3	
Land Cover	Snow/Ice	5	0.03
	Other (Rocky, Barren, Marines, etc.)	3	

Table 6. MCDA-AHP approach pairwise comparison matrix with weight values for each layer.

Layers	S	C	A	TR	E	LC	Weight Value
S	1	2	3	5	7	9	0.404
C	1/2	1	3	4	5	7	0.281
A	1/3	1/3	1	2	3	5	0.143
TR	1/5	1/4	1/2	1	2	3	0.085
E	1/7	1/5	1/3	1/2	1	2	0.054
LC	1/9	1/7	1/5	1/3	1/2	1	0.033
Consistency Ratio							0.0178

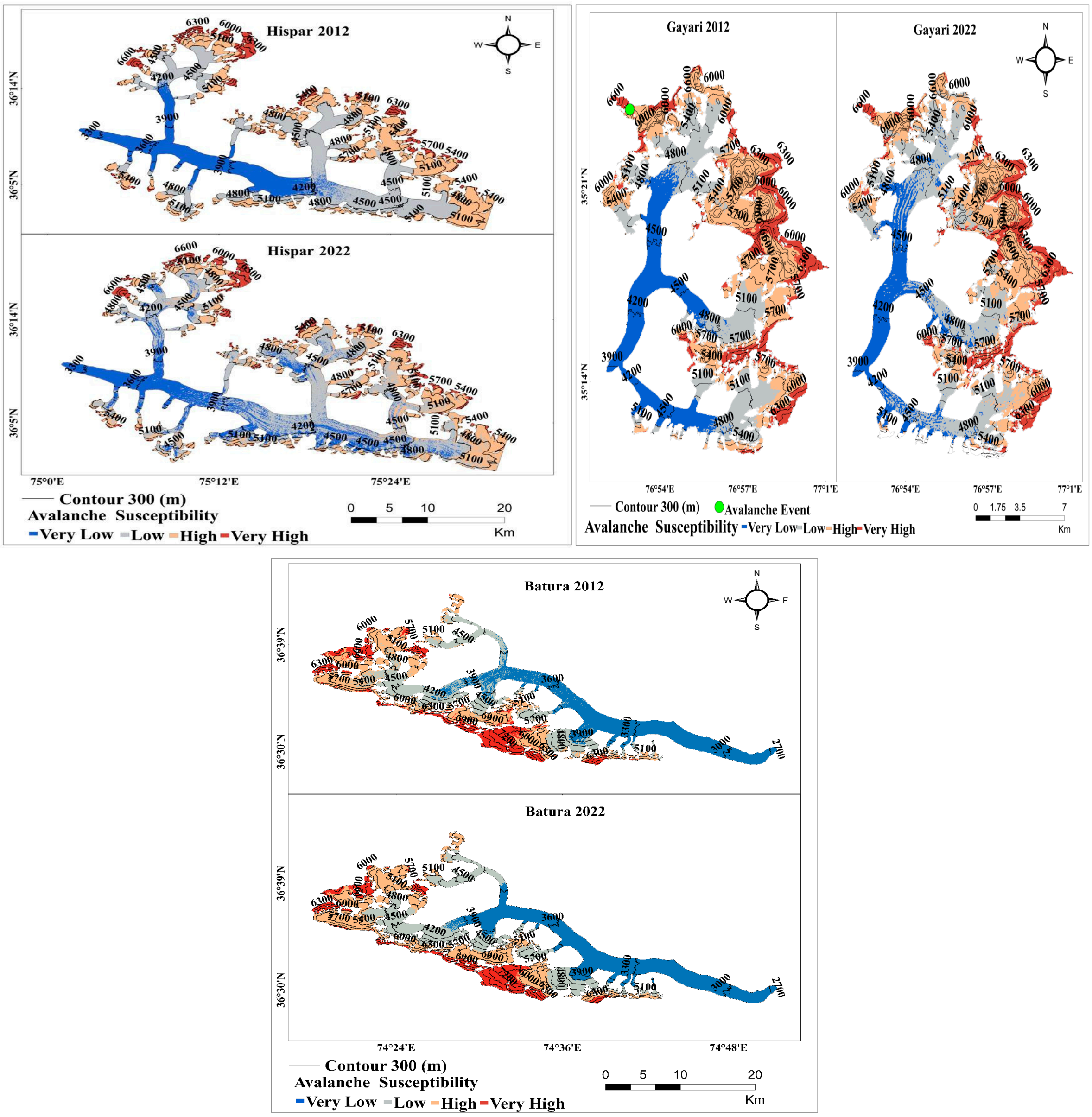

Figure 7. Snow avalanche susceptibility of Hispar, Gayari, and Batura Glaciers for 2012 and 2022.

Another factor is the aspect in which classes in the north and southeast are thought to be more vulnerable to avalanche occurrence. Table 7 below reveals a significant increase in susceptibility to snow avalanches in 2022 compared to 2012, as indicated by the susceptibility percentages (53%). This heightened vulnerability can be attributed to diverse meteorological influences and the impact of climate change over the past decade. The application of snow avalanche susceptibility mapping through satellite remote sensing employing the Analytic Hierarchy Process (AHP) technique has proven instrumental in discerning these shifts, enabling a more comprehensive understanding of avalanche dynamics, and emphasizing the pressing need for adaptive measures in affected regions. To compare the susceptibility, we selected Hispar, Batura, and Gayari Sector Glaciers as our expanded areas of interest.

Table 7. The table represents the area and percentage of Hispar Glacier for 2012 and 2022.

Glacier	Classes	Area km^2	Percentage
Hispar 2012	Very low	50.3	12.65
	Low	28.61	7.20
	High	136.61	34.37
	Very high	182.01	45.76
Hispar 2022	Very low	52.71	13.25
	Low	25.03	6.29
	High	106.95	26.92
	Very high	212.84	53.52

The ASI is divided into four susceptibility perimeters, which are as follows: very low, low, high, and very high (Figure 7). South and north aspect classifications are thought to be more prone to avalanche occurrence. The slope's peaks, in contrast to areas of evident slope peaks and low slopes, are the key factors in avalanche susceptibility zones. Also, the slope with peaks is the major component in avalanche hazard, as opposed to the location where the slope peaks are not visible and there is an exceptionally low slope. Contour lines show the elevation of Batura Glaciers, as shown in Figure 7b. Table 8 shows very low, low, high, and very high susceptibility with the area and the percentage of Batura Glacier. In 2012, low susceptibility was 6.06%, and very high susceptibility was 48.46%, as shown in Table 8. In 2022, the very highly susceptible area was 40.41%.

Table 8. The table represents the area and percentage of Batura Glacier for 2012 and 2022.

Glacier	Classes	Area km^2	Percentage
Batura 2012	Very low	16.24	13.08
	Low	7.46	6.06
	High	40.70	33.56
	Very high	60.57	48.46
Batura 2022	Very low	10.04	15.95
	Low	20.18	7.93
	High	45.11	35.67
	Very high	51.11	40.41

The Gayari avalanche is situated at an extremely high altitude and is challenging to reach, as well as being close to the borders between India and China in Pakistan's far northeast. The existence of a decent slope as well as the formation of a small thickness are, indeed, the two primary avalanche-causing conditions. Snow accumulation in the Gayari region meets both criteria: slope (35–50°) and crack activity were detected in 2012 at approximately 900 m elevation upstream from either glacier terminal. Consequently, susceptibility was greater in 2012 than in 2022, as shown in Figure 7c. The green dots in this figure represent the serious avalanche event that happened on 7 April 2012 in the Gayari Sector near Siachen Glacier, causing 129 soldier and 11 civilian causalities. Contour lines show the elevation of the area. The most susceptible area in 2012 was 60.57 km^2 with 48.46% susceptibility, as shown in Table 9.

Table 9. The area and percentage of Gayari Glacier for 2012 and 2022.

Glacier	Classes	Area km^2	Percentage
Gayari 2012	Very low	16.24	13.08
	Low	7.46	6.06
	High	40.70	33.56
	Very high	60.57	48.46
Gayari 2022	Very low	10.04	15.95
	Low	20.18	7.93
	High	45.11	35.67
	Very high	51.11	40.41

4. Discussion

The study area is exceptionally complicated; steep slopes, insufficient accessibility, and severe weather conditions make it extremely challenging to map avalanche susceptibility in the region. Human actions and decisions govern the fatal avalanche patterns in high mountains [5] that contributed to about three-quarters of the avalanche deaths due to improper camp placements and failure to forecast snow avalanches. The main components affecting the avalanche formation were determined as slope, elevation, aspect, vegetation index, and curvature profile, and then these parameters were arranged hierarchically according to the literature and nature of the study area [6,7]. However, a parameter value may dominantly affect the occurrence of a snow avalanche while the effect of the other parameter may disappear on the snow avalanche occurrence [8]. Thus, it is not easy to conclude the exact criteria for such a complicated fact of nature [9]. The avalanche hazards and frequency in the study area, especially in the Batura and Gayari Glaciers, are common and cause huge losses of life and infrastructure as the Karakoram Highway lies in the region that connects the ancient Silk Road and serves as a vital transportation route in Pak China Economic Corridor (CPEC) and is critical to the economic development of the country. The AHP approach is commonly used for decision-making and is broadly utilized in natural hazard situations [31–35]. According to the classification study and AHP technique, in 2012, Gayari was declared as the most susceptible glacier, while in 2012, Hispar was the second most avalanche-suspectable glacier. Batura had moderate susceptibility in 2012 and 2022 (Figure 7). The current study was preceded by several processes, including the creation of a snow avalanche inventory map, production and analysis of avalanche occurrence terrain characteristics, the building of a pairwise comparison matrix, the estimation of variable weighting factors, and susceptibility mapping.

The results also showed that the slope factor had the maximum weight value [11,36], and ignorance of the behavior of the avalanche slopes could be the main reason for the avalanche accidents in the region [37], while other factors like terrain roughness, aspect, and curvature also contributed; however, most of these are essential factors, and they are constant over time [6,9]. Land cover and elevation were found to have low significant contributing values and relevant avalanche vulnerability variables.

Limitations and Future Prospective of Avalanches Susceptibility Mapping

Important snowpack data sets needed for avalanche susceptibility mapping include snow depth, snowpack density, snow layer thickness and interfaces, snowpack temperature, snowpack hardness, snow crystal types, and snowpack stability, along with historical avalanche data and weather data. However, due to several limitations, we were not able to integrate and analyze these diverse data sets for avalanche mapping. This includes spatial variability as snowpack conditions vary significantly over short distances, and this spatial variability can lead to large uncertainties and temporal and spatial data gaps concerning the mapping of avalanche activity [38] if based on limited data points. [39] identified similar challenges with observation networks. This inaccessibility of the areas of the Himalayas and Karakoram ranges is more complex due to its dynamic geomorphology/geosystem [40]. The most important is a limitation of equipment and sensors due to resource constraints, resulting in unavailability or limited availability of data in most of such regions, including our study area. There is no single weather station installed in the study area as harsh environments and limited accessibility pose challenges for establishing meteorological and ground monitoring stations [41]. Despite the challenges, ongoing research and advancements in technology continue to enhance our understanding of snowpack conditions and avalanche risk. Currently, remote sensing technology has made significant strides over the past few decades, emerging as the principal approach for large-scale and high-precision snow monitoring, providing an improved quantitative measure of avalanche activity and dynamics. To overcome such limitations, scientists often use a combination of field observations, remote sensing data, and advanced computer modeling, which include both statistical models that interpret available data and physical models that generate new data that would otherwise not be available from field observations to improve the accuracy of avalanche forecasting and mapping.

Future research should be focused on dealing with the detection of small avalanches and the differentiation between slab and loose snow avalanches, as well as between wet and dry snow avalanches. These challenges can be achieved from a combination of new sensor systems, improved automatic avalanche detection methods, and an improved understanding of the electromagnetic properties of snow in avalanche debris. The technical integration of remote sensing data into operational avalanche forecasting is seen as the next future challenge.

5. Conclusions

The AHP model based on GIS has been proven to be appropriate for mapping the avalanche susceptibility of glaciers in the Karakoram range of Pakistan, which has more glacial ice than any other country on Earth outside the polar regions. The results confirm that the region has hotspots with high risks of avalanche development and related disasters. Overall, more than 50% of areas have high susceptibility. As the region is a tourist area and construction is increasing rapidly, it will be appropriate to implement precautionary measures and develop mitigation strategies, and local governments, especially, should make proper preparedness plans in case of any disaster. Such a map cannot prevent avalanches; however, its appropriate use may decrease avalanche casualties. Decision makers may utilize this avalanche susceptibility map to optimize planning and management and secure mobility throughout the area. Regrettably, this study encounters limitations due to the unavailability of snow characteristics data in the study area, especially avalanche conditioning factors. The collection of dynamic meteorological characteristics would be useful for even more specific and accurate mapping along with the integration of snowpack characteristics like seismic setting, faults, geology, flood, and other anthropogenic factors in future studies, which was not possible in current work due to the unavailability of data. Not even a single ground weather station was available, and this is a big concern that needs to be addressed by governments and other relevant organizations. In our future research, the scope of the study will be expanded to investigate the avalanche hazard risk considering all these characteristics.

Author Contributions: Conceptualization, A.R.; methodology, A.R.; software, M.Y.S.D.; validation, A.R., M.Y.S.D. and Z.A.S.; writing—original draft preparation, A.R. and B.U; writing—review and editing, B.U.; visualization, F.A.A.; supervision, Z.A.S.; funding acquisition, E.A.A.I. and F.A.A. All authors have read and agreed to the published version of the manuscript.

Funding: This project is funded by King Saud University, Riyadh, Saudi Arabia.

Data Availability Statement: The data presented in this study are available on request from the corresponding author.

Acknowledgments: Researchers supporting project number (RSPD2023R576), King Saud University, Riyadh, Saudi Arabia.

Conflicts of Interest: The authors declare no conflict of interest.

References

1. Shahzad, L.; Tahir, A.; Sharif, F.; Khan, W.U.D.; Farooq, M.A.; Abbas, A.; Saqib, Z.A. Vulnerability well-being, and livelihood adaptation under changing environmental conditions: A case from mountainous region of Pakistan. *Environ. Sci. Pollut. Res.* **2019**, *26*, 26748–26764. [CrossRef]
2. Kumar, S.; Srivastava, P.K.; Snehmani. GIS-based MCDA–AHP modelling for avalanche susceptibility mapping of Nubra valley region, Indian Himalaya. *Geocarto Int.* **2017**, *32*, 1254–1267. [CrossRef]
3. Varol, N. Avalanche susceptibility mapping with the use of frequency ratio, fuzzy and classical analytical hierarchy process for Uzungol area, Turkey. *Cold Reg. Sci. Technol.* **2021**, *194*, 103439. [CrossRef]
4. Bası, M.P.; Pereira, V.; Costa, H.G.; Santos, M.; Ghosh, A. A systematic review of the applications of multi-criteria decision aid methods (1977–2022). *Electronics* **2022**, *11*, 1720.
5. McClung, D.M. Avalanche character and fatalities in the high mountains of Asia. *Ann. Glaciol.* **2016**, *57*, 114–118. [CrossRef]
6. Yilmaz, B. Application of GIS-Based Fuzzy Logic and Analytical Hierarchy Process (AHP) to Snow Avalanche Susceptibility Mapping. Master's Thesis, University of Colorado Boulder, North San Juan, CO, USA, 2016.
7. Kumar, S.; Srivastava, P.K.; Snehmani. Geospatial modelling and mapping of snow avalanche susceptibility. *J. Indian Soc. Remote. Sens.* **2018**, *46*, 109–119. [CrossRef]
8. Christophe, C.; Georges, R.; Jérôme, L.S.; Markus, S.; Pascal, P. Spatio-temporal reconstruction of snow avalanche activity using tree rings: Pierres Jean Jeanne avalanche talus, Massif de l'Oisans, France. *Catena* **2010**, *83*, 107–118. [CrossRef]
9. Akay, H. Spatial modeling of snow avalanche susceptibility using hybrid and ensemble machine learning techniques. *CATENA* **2021**, *206*, 105524. [CrossRef]
10. Khan, H.; Vasilescu, L.G.; Khan, A. Disaster management cycle-a theoretical approach. *J. Manag. Mark.* **2008**, *6*, 43–50.
11. Mosavi, A.; Shirzadi, A.; Choubin, B.; Taromideh, F.; Hosseini, F.S.; Borji, M.; Shahabi, H.; Salvati, A.; Dineva, A.A. Towards an ensemble machine learning model of random subspace based functional tree classifier for snow avalanche susceptibility mapping. *IEEE Access* **2020**, *8*, 145968–145983. [CrossRef]
12. Statham, G.; Haegeli, P.; Greene, E.; Birkeland, K.; Israelson, C.; Tremper, B.; Stethem, C.; McMahon, B.; White, B.; Kelly, J. A conceptual model of avalanche hazard. *Nat. Hazards* **2018**, *90*, 663–691. [CrossRef]
13. Yariyan, P.; Avand, M.; Abbaspour, R.A.; Karami, M.; Tiefenbacher, J.P. GIS-based spatial modeling of snow avalanches using four novel ensemble models. *Sci. Total. Environ.* **2020**, *745*, 141008. [CrossRef]
14. Yang, J.; He, Q.; Liu, Y. Winter–spring prediction of snow avalanche susceptibility using optimisation multi-source heterogeneous factors in the Western Tianshan Mountains, China. *Remote. Sens.* **2022**, *14*, 1340. [CrossRef]
15. Snehmani; Bhardwaj, A.; Pandit, A.; Ganju, A. Demarcation of potential avalanche sites using remote sensing and ground observations: A case study of Gangotri glacier. *Geocarto Int.* **2014**, *29*, 520–535. [CrossRef]
16. Snehmani; Dharpure, J.K.; Kochhar, I.R.; Hari Ram, P.; Ganju, A. Analysis of snow cover and climatic variability in Bhaga basin located in western Himalaya. *Geocarto Int.* **2016**, *31*, 1094–1107. [CrossRef]
17. Singh, D.K.; Gusain, H.S.; Mishra, V.; Gupta, N. Snow cover variability in North-West Himalaya during last decade. *Arab. J. Geosci.* **2018**, *11*, 579. [CrossRef]
18. Singh, D.K.; Mishra, V.D.; Gusain, H.S.; Gupta, N.; Singh, A.K. Geo-spatial modeling for automated demarcation of snow avalanche hazard areas using Landsat-8 satellite images and in situ data. *J. Indian Soc. Remote. Sens.* **2019**, *47*, 513–526. [CrossRef]
19. Singh, D.K.; Gusain, H.S.; Mishra, V.; Gupta, N.; Das, R.K. Automated mapping of snow/ice surface temperature using Landsat-8 data in Beas River basin, India, and validation with wireless sensor network data. *Arab. J. Geosci.* **2018**, *11*, 136. [CrossRef]
20. Selcuk, L. An avalanche hazard model for Bitlis Province, Turkey, using GIS based multicriteria decision analysis. *Turk. J. Earth Sci.* **2013**, *22*, 523–535. [CrossRef]
21. Sardar, T.; Raziq, A.; Rashid, A.; Saddiq, G. Snow avalanche-based susceptibility assessment of selected districts in northern zone of Pakistan applying MCDA approach in GIS. *J. Himal. Earth Sci.* **2019**, *52*, 64–73.
22. Sappington, J.M.; Longshore, K.M.; Thompson, D.B. Quantifying landscape ruggedness for animal habitat analysis: A case study using bighorn sheep in the Mojave Desert. *J. Wildl. Manag.* **2007**, *71*, 1419–1426. [CrossRef]
23. Saaty, T.L. *What is the Analytic Hierarchy Process?* Springer: Berlin/Heidelberg, Germany, 1988.
24. Saaty, T.L. Decision Making with the Analytic Hierarchy Process. *Int. J. Serv. Sci.* **2008**, *1*, 83–98. [CrossRef]
25. Saaty, R.W. The analytic hierarchy process—What it is and how it is used. *Math. Model.* **1987**, *9*, 161–176. [CrossRef]
26. Parshad, R.; Kumar, P.; Snehmani; Srivastva, P.K. Seismically induced snow avalanches at Nubra–Shyok region of Western Himalaya, India. *Nat. Hazards* **2019**, *99*, 843–855. [CrossRef]
27. Mouginot, J.; Rignot, E.; Scheuchl, B.; Millan, R. Comprehensive annual ice sheet velocity mapping using Landsat-8, Sentinel-1, and RADARSAT-2 data. *Remote. Sens.* **2017**, *9*, 364. [CrossRef]
28. Mahboob, M.A.; Iqbal, J.; Atif, I. Modeling and simulation of glacier avalanche: A case study of gayari sector glaciers hazards assessment. *IEEE Trans. Geosci. Remote. Sens.* **2015**, *53*, 5824–5834. [CrossRef]
29. Landrø, M.; Pfuhl, G.; Engeset, R.; Jackson, M.; Hetland, A. Avalanche decision-making frameworks: Classification and description of underlying factors. *Cold Reg. Sci. Technol.* **2020**, *169*, 102903. [CrossRef]
30. Kumar, S.; Srivastava, P.K.; Bhatiya, S. Geospatial probabilistic modelling for release area mapping of snow avalanches. *Cold Reg. Sci. Technol.* **2019**, *165*, 102813. [CrossRef]

31. Kumar, S.; Snehmani; Srivastava, P.K.; Gore, A.; Singh, M.K. Fuzzy–frequency ratio model for avalanche susceptibility mapping. *Int. J. Digit. Earth* **2016**, *9*, 1168–1184. [CrossRef]
32. Karim, R.; Tan, G.; Ayugi, B.; Babaousmail, H.; Liu, F. Evaluation of historical CMIP6 model simulations of seasonal mean temperature over Pakistan during 1970–2014. *Atmosphere* **2020**, *11*, 1005. [CrossRef]
33. Sarhangi, E.J.; Lorestani, G.; Falah, V. Avalanche Hazard Zoning Using LNRF and Shannon Entropy Models Case Study: Part of Haraz Road, Poldokhtar-Vana. *Hydrogeomorphology* **2023**, *10*, 66–81.
34. Giacona, F.; Eckert, N.; Corona, C.; Mainieri, R.; Morin, S.; Stoffel, M.; Martin, B.; Naaim, M. Upslope migration of snow avalanches in a warming climate. *Proc. Natl. Acad. Sci. USA* **2021**, *118*, e2107306118. [CrossRef] [PubMed]
35. Hewitt, K. *Regions of Risk: A Geographical Introduction to Disasters*; Routledge: London, UK, 2014.
36. Ganju, A.; Thakur, N.K.; Rana, V. Characteristics of avalanche accidents in western Himalayan region, India. In Proceedings of the International Snow Science Workshop, Penticton, BC, Canada, 29 September–4 October 2002; pp. 200–207.
37. Germain, D. Snow avalanche hazard assessment and risk management in northern Quebec, eastern Canada. *Nat. Hazards* **2015**, *80*, 1303–1321. [CrossRef]
38. Atkins, D. *Snow, Weather, and Avalanches: Observational Guidelines for Avalanche Programs in the United States*; American Avalanche Association: Bozeman, MT, USA, 2010.
39. Lundquist, J.; Hughes, M.; Gutmann, E.; Kapnick, S. Our skill in modeling mountain rain and snow is bypassing the skill of our observational networks. *Bull. Am. Meteorol. Soc.* **2019**, *100*, 2473–2490. [CrossRef]
40. Rawat, M.; Karwariya, S.; Raushan, R.; Kanga, S.; Taloor, A.K.; Thapliyal, A. Snow cover and land surface temperature assessment of Mana basin Uttarakhand India using MODIS satellite data. In *Water, Cryosphere, and Climate Change in the Himalayas: A Geospatial Approach*; Springer: Berlin/Heidelberg, Germany, 2021; pp. 159–174.
41. Xi, N.; Mei, G. Avalanche Susceptibility Mapping by Investigating Spatiotemporal Characteristics of Snow Cover Based on Remote Sensing Imagery along the Pemo Highway—A Critical Transportation Road in Tibet, China. *Water* **2023**, *15*, 2743. [CrossRef]